

CHEMISTRY

A European Journal

A Journal of



Accepted Article

Title: Constructive Quantum Interference in Single-Molecule Benzodichalcogenophene Junctions

Authors: Colin John Lambert, Masoud Baghernejad, Yang Yang, Oday Al Owaedi, Yyves Aeshchi, Biao-Feng Zeng, Zahra Dawood, Xiaohui Li, Junyang Liu, Jia Shi, Silvio Decurtins, Shi-Xia Liu, and Wenjing Hong

This manuscript has been accepted after peer review and appears as an Accepted Article online prior to editing, proofing, and formal publication of the final Version of Record (VoR). This work is currently citable by using the Digital Object Identifier (DOI) given below. The VoR will be published online in Early View as soon as possible and may be different to this Accepted Article as a result of editing. Readers should obtain the VoR from the journal website shown below when it is published to ensure accuracy of information. The authors are responsible for the content of this Accepted Article.

To be cited as: *Chem. Eur. J.* 10.1002/chem.201905878

Link to VoR: <http://dx.doi.org/10.1002/chem.201905878>

Supported by
ACES

WILEY-VCH

Constructive Quantum Interference in Single-Molecule Benzodichalcogenophene Junctions

Masoud Baghernejad^[a, c], Yang Yang^[a], Oday A. Al-Owaedi^[b], Yves Aeschi^[c], Biao-Feng Zeng^[a], Zahra Murtada Abd Dawood^[b], Xiaohui Li^[a], Junyang Liu^[a], Jia Shi^[a], Silvio Decurtins^[c], Shi-Xia Liu^[c], Wenjing Hong^[a, c] and Colin J. Lambert^[d]

This manuscript is dedicated to the memory of Professor Thomas Wandlowski.

Abstract: Heteroatom substitution into the cores of alternant, aromatic hydrocarbons containing only even-membered rings is attracting increasing interest as a method of tuning their electrical conductance. Here we examine the effect of heteroatom substitution into molecular cores of non-alternant hydrocarbons, containing odd-membered rings. Benzodichalcogenophene (BDC) compounds are rigid, planar π -conjugated structures, with molecular cores containing 5-membered rings fused to a 6-membered aryl ring. To probe the sensitivity or resilience of constructive quantum interference (CQI) in these non-bipartite molecular cores, two C_2 -symmetric molecules (I

and II) and one asymmetric molecule (III) are investigated. I (II) contains S (O) heteroatoms in each of the 5-membered rings, while III contains an S in one 5-membered ring and an O in the other. Differences in their conductances arise primarily from the longer S-C and shorter O-C bond lengths compared with the C-C bond and the associated changes in their resonance integrals. We find that although the conductance of III is significantly lower than the conductances of the others, CQI is resilient and persists in all molecules.

Introduction

When a single molecule is connected to source and drain electrodes, the electrical conductance of the resulting device is controlled by the quantum interference (QI) pattern within the molecule, created by de Broglie waves of electrons injected into the molecule by the source.^[1] Stimulated by the desire to develop molecular-scale diodes,^[2-4] transistors,^[5,6] switches^[7-10] and thermoelectric devices^[11-13] with improved performance, recent effort has been devoted to exploiting such wave patterns within heterocyclic aromatic molecules. Polyaromatic hydrocarbons (PAHs) and their derivatives are particularly attractive, because they contain multiple interfering pathways, which promote QI and can be influenced by external electrostatic or electrochemical gating,^[14] by varying their connectivities to external electrodes^[15,16] or by heteroatom substitution.^[17] When the core of a graphene-like PAH is weakly coupled to external electrodes by atoms i and j , the single-molecule electrical conductance σ_{ii} depends on the choice of

connecting atoms i, j .^[11] Furthermore, unless a molecule is electrostatically or electrochemically gated, the highest occupied and lowest unoccupied molecular orbitals (HOMO and LUMO, respectively) levels adjust themselves such that the Fermi energy of the electrodes lies in the vicinity of the middle of the HOMO-LUMO gap.^[18,19] Consequently, if the core of the molecule is weakly coupled to the electrodes (e.g., via triple bonds, which link the core to an anchoring group), the electrical conductance is proportional to $(g_{ii})^2$, where g_{ii} is the amplitude of an electronic de Broglie wave on atom j , due to electrons injected into the core at site i with energies close to the middle of the HOMO-LUMO gap. These concepts of weak coupling, connectivity and mid-gap transport have been utilised in a series of papers to develop quantum circuit rules for materials discovery and to develop a simple magic ratio rule (MRR)^[15] for describing the influence of connectivity on QI in heterocyclic PAHs.

With a view to optimising transport through PAH-based molecular junctions, it is of interest to investigate how such wave patterns are modified by heteroatom substitution. If the modification is not too strong, then starting from a “parent” graphene-like PAH, such a study would allow the electrical conductance of a “daughter” heteroatom-substituted molecule to be predicted using simple perturbation theory. For bipartite, aromatic, parental cores, in which odd-numbered sites are connected to even-numbered sites only, a recent study revealed simple rules governing the effect of heteroatom substitution, which were verified by comparison with density functional theory and by experiments on heteroatom-substituted oligo(phenylene-ethynylene) compounds.^[17,20] Our aim is to investigate the effect of heteroatom substitution when the parent is a non-bipartite, aromatic molecule, stimulated in part by a desire to understand electron transport through benzodichalcogenophene (BDC) compounds, which possess a rigid and planar π -conjugated structure with strong electron donating ability.^[21,22] These properties have led to their use as organo-electronic compounds in dye-sensitized solar cells (DSSC), field effect transistors (OFET), organic light-

- [a] Dr. Masoud Baghernejad, Dr. Yang Yang, Dr. Biao-Feng Zeng, Dr. Xiaohui Li, Junyang Liu, Dr. Jia Shi, Prof. Wenjing Hong. State Key Laboratory of Physical Chemistry of Solid Surfaces, Pen-Tung Sah Institute of Micro-Nano Science and Technology, College of Chemistry and Chemical Engineering, iChEM, Xiamen University, 361005, Xiamen, China
E-mail: whong@xmu.edu.cn
- [b] Dr. Oday A. Al-Owaedi, Zahra Murtada Abd Dawood. Department of Laser Physics, Women Faculty of Science, the University of Babylon, Hilla 51001, Iraq.
E-mail: oday.alowaedi@gmail.com
- [c] Dr. Masoud Baghernejad, Dr. Yves Aeschi, Prof. Wenjing Hong, Prof. Silvio Decurtins, Dr. Shi-Xia Liu. Department of Chemistry and Biochemistry, University of Bern, Freiestrasse 3, 3012 Bern, Switzerland.
Email: liu@dcb.unibe.ch
- [d] Prof. Colin J. Lambert. Department of Physics, University of Lancaster, Lancaster, LA1 4YB, UK.
Email: c.lambert@lancaster.ac.uk

emitting diodes (OLED) and in charge transport studies of single molecules.^[23-29] However the non-bipartite nature of the central core, the non-uniform bonding geometry and structural rearrangement of typical anchoring groups in the junction, complicates the interpretation of charge transport data. Improvement has been achieved through the use of alternative and rather high conductance carbon-gold anchoring using trimethylsilyl-protected compounds, which facilitate a rather more robust data interpretation.^[30,31] However, the role of QI within the non-bipartite, aromatic core has not been extensively addressed.

In the present paper, charge transport properties of three BDC compounds **I** (SS), **II** (OO) and **III** (SO) (Figure 1) have been investigated using a scanning tunneling microscopy-break junction (STM-BJ). These molecules allow us to examine the relative effect of C₂-symmetric and asymmetric chalcogen substitution in BDC-compounds. We demonstrate that although all of them exhibit constructive quantum interference (CQI), the asymmetric **III** (SO) has a conductance value several times lower than those of the symmetric **I** (SS) and **II** (OO). These experimental results are verified by a combination of density functional theory (DFT), tight binding (Hückel) modelling and perturbation theory.

Results and Discussion

The target compounds **I-III** were prepared according to literature methods.^[21] The single-molecule conductance measurements were carried out in a THF/mesitylene solution (1:4, v/v) containing 0.1 mM target compound and tetrabutylammonium fluoride (TBAF, 4 equivalents) using STM-BJ techniques, as sketched in Figure 1.^[32] Our previous work^[31] has demonstrated that the stable molecular junctions can be formed via the covalent bonds between gold electrodes and alkynylides generated by *in-situ* desilylation in the presence of TBAF.

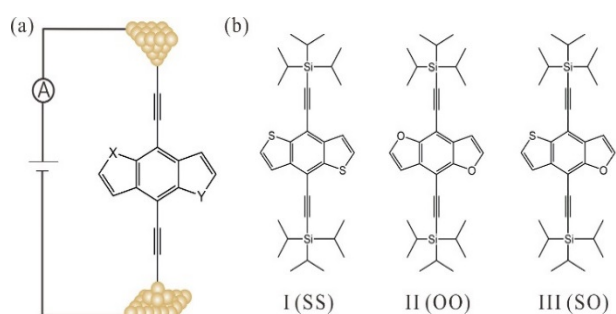


Figure 1. (a) Schematics of STM-BJ measurement. (b) Chemical structures of compounds **I** (SS), **II** (OO), and **III** (SO).

As shown in Figure 2a-c, the typical conductance-distance traces (in units of the conductance quantum $G_0 = 2e^2/h$) from the conductance measurements of BDC-molecules show a well-defined plateau in the range of $\log(G/G_0)$ around -3.6 for compounds **I** (SS) and **II** (OO), and around -3.9 for compound **III** (SO), which we assign to the conductance of single-molecule junctions. The two-dimensional (2D) conductance histograms (Figure 2d-f) show features of gold atomic contacts around $G \geq 1$

G_0 followed by a cloud-like plateau in the range $[10^{-4.6} G_0 < G < 10^{-3.2} G_0]$, centered at $G = 10^{-3.9} G_0$ for compound **III** (SO) and $G = 10^{-3.6} G_0$ for compounds **I** (SS) and **II** (OO).

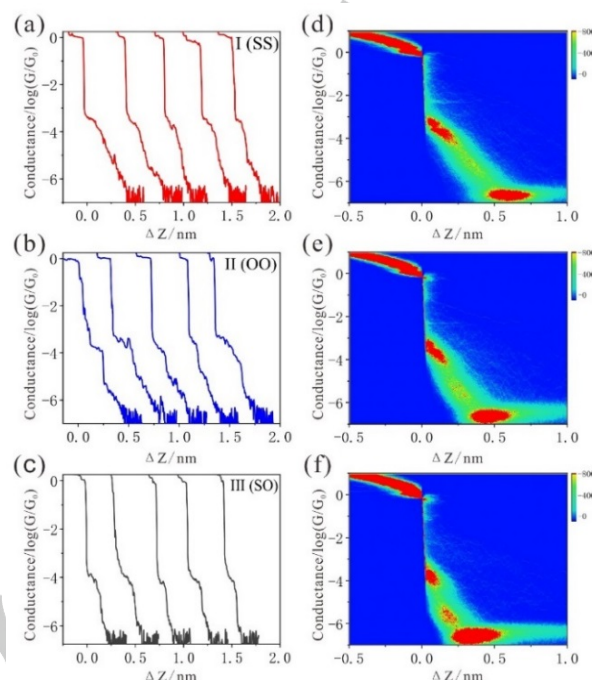


Figure 2. (a-c) Typical conductance-distance traces and (d-f) two-dimensional histograms of compounds **I** (SS), **II** (OO), and **III** (SO). The histograms are constructed from more than 4000 single current-distance traces without data selection.

The cloud-like plateau in 2D histogram leads to the peak in the one-dimensional (1D) conductance histogram that constructed from more than 4000 individual traces without any data selection, as shown in Figure 3. This is attributed to the formation of single-molecule junction. As shown by our theoretical modelling below, this trend in conductances is a reflection of the fact that the LUMO orbitals of compounds **I** (SS) and **II** (OO) are shifted to lower and higher energies respectively relative to compound **III** (SO). In addition, the lengths of the S-C and O-C bonds are $L_{S-C} = 0.174$ nm and $L_{O-C} = 0.136$ nm, which are longer and shorter respectively than the length of the C-C bond ($L_{C-C} = 0.144$ nm), leading to smaller and larger resonance integrals between the heteroatoms on their neighboring carbons. Our theoretical modelling reveals that the latter effect rather than the level shift of the LUMOs leads to the lower conductance of compound **III** (SO) compared with compounds **I** (SS) and **II** (OO).

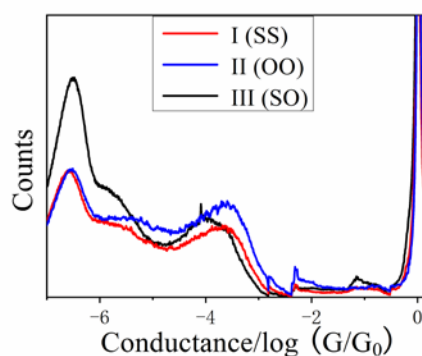


Figure 3. One-dimensional conductance histograms of compounds **I** (SS), **II** (OO), and **III** (SO).

To better understand the conductance behavior, the electronic properties of the molecules and electrical behavior of the junctions were investigated using DFT-based theory and tight-binding methods.^[33] Initial studies of the electronic structures of all molecules were carried out at B3LYP level of theory^[34] with 6-31G**³ basis set. Figure 4 gives the plots of the HOMOs and LUMOs. These orbitals are real functions and have either a positive or negative^[35,36] sign. Crucially, the sign of the HOMOs on the left acetylene linker are of opposite to the sign on the right acetylene linker, whereas the LUMOs have the same sign on the left and right acetylene linkers. As discussed previously,^[35] this means that for each molecule, the HOMO orbital product is negative and the LUMO orbital product is positive. Therefore, their inter-orbital quantum interference is constructive within the HOMO-LUMO gap. Figure 4 shows that the HOMOs of all molecules are extended over the BDC backbone. The LUMOs exhibit a negligible weight on the S or O atoms and are therefore are less delocalized than the HOMOs.

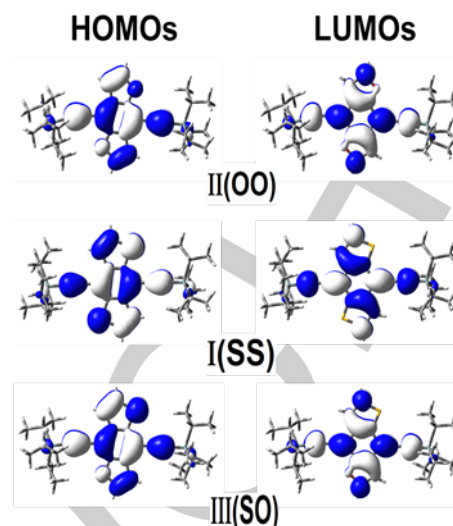


Figure 4. Plots of the HOMO and LUMO of all molecules (iso-surfaces ± 0.02 (e/bohr^3)^{1/2}).

Figure 5a shows the relaxed geometries of the molecules within the gold junctions and Figure 5b shows their corresponding transmission coefficients, from which their electrical conductance is given by $G = G_0 T(E_F)$, where G_0 is the conductance quantum. As expected from Hückel theory (see Supporting Information), the LUMO transmission resonances (near $E = 2.3$ eV) of the II (OO) and I (SS) molecules respectively lie above and below that of the III (SO) molecule. Furthermore, as expected, since the HOMO and LUMO orbital

products are of opposite sign, interference is constructive^[35] and there is no destructive interference feature within the gap. A key factor governing the conductance of a molecular junction is the position of the Fermi level of a metal electrode with respect to the molecular HOMO and LUMO levels. In turn this energy alignment is sensitive to the chemical nature of the contacting groups, which bind the molecule to the electrode, and also the precise configuration of the metal electrode-molecule contact.^[37-42] To determine E_F , the predicted conductance values of all molecules were compared with the experimental values and a single common value of E_F was chosen, which gave the closest overall agreement. This yielded a value of $E_F - E_F^{\text{DFT}} = 1.0$ eV, which is used in all of the DFT results described below. The experimental data now is interpreted with the aid of Figure 5b, which indicates that in all cases the Fermi level lies close to the middle of the HOMO-LUMO gap and transport takes place via non-resonant tunneling.^[43-45] Table 1 shows a comparison between experimental and theoretical conductances, along with other relevant junction parameters.

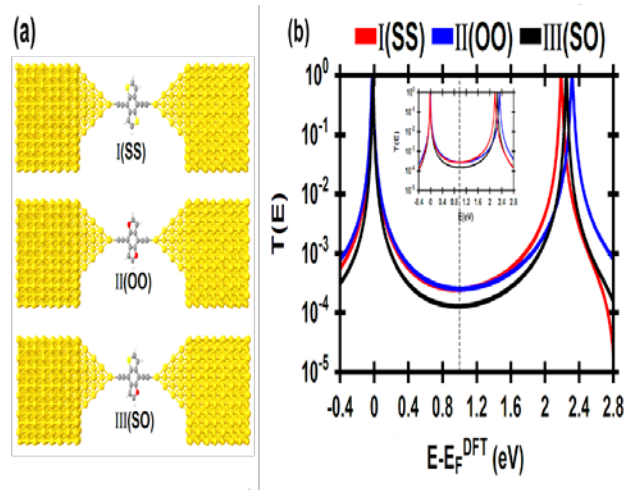


Figure 5. (a) The relaxed geometries of molecular junctions of I (SS), II (OO), and III (SO). (b) The transmission functions for all molecular junctions. Black dashed line shows the chosen Fermi energy ($E_F - E_F^{\text{DFT}} = 1$ eV). The insert shows the result of a tight binding calculation (see Supporting Information) based on a minimal Hückel description of transport through the cores of the molecules.

Table 1. The experimental (Exp. G/G_0) and calculated conductance values (Th. G/G_0) at $E - E_F^{\text{DFT}} = 1.0$ eV. The calculated electrode separation in the relaxed junctions (Z); $Z = d_{\text{Au-Au}} - 0.25$ nm, where 0.25 nm is the calculated center-to-center distance of the apex atoms of the two opposing gold pyramids when the conductance equals G_0 in the absence of a molecule. $d_{\text{Au-Au}}$ is the calculated center-to-center distance of the apex atoms of the two opposing gold pyramids in relaxed junctions. Molecular length (d) is the distance between the centres of anchor atoms in relaxed junction. Bond length (X) is the distance between the top gold atoms of the pyramids and the anchor atoms in relaxed junctions. ΔE (eV) is the binding energy of the molecules to the electrodes.

Molecule	Exp. G/G ₀	Th. G/G ₀	Z nm	d _{Au-Au} nm	d nm	X nm	ΔE (eV)
SS	2.512×10 ⁻⁴	2.528×10 ⁻⁴	0.991	1.241	0.817	0.212	-3.3
OO	2.512×10 ⁻⁴	2.528×10 ⁻⁴	0.994	1.244	0.821	0.212	-3.4
SO	1.258×10 ⁻⁴	1.291×10 ⁻⁴	0.992	1.242	0.819	0.212	-3.02

To understand the relative effect of the S and O heteroatoms, we constructed a minimal tight-binding (Hückel) representation of the “parental” core of the molecules before heteroatom substitution shown in Figure 6 and then considered the effect of heteroatom substitution to yield the “daughters” shown in Figure 5a. The simplest tight-binding Hamiltonian of the parent is obtained by assigning a site energy ε_0 to each diagonal and a nearest neighbor hopping integral $-\gamma$ between neighbouring sites, i.e., $H_{ii} = \varepsilon_0$ and $H_{ij} = -\gamma$ if i, j are nearest neighbours. A minimal model of the heteroatom-substituted “daughters” is then obtained simply by shifting the site energies of sites 3 and 9 to accommodate the different electronegativities of O and S, leading to first-order shifts in their LUMOs and a negligible shift in their HOMOs (see SI for a detailed analysis). However, as shown in Figure S3 of the SI, such shifts alone are not sufficient to yield agreement with the DFT results and experiments, and would not yield a lower value of conductance for the asymmetric molecule. On the other hand, if the O-C and S-C hopping integrals are adjusted to account for the differences in lengths between the O-C bond (0.136 nm), the S-C bond (0.174 nm) compared with the C-C bonds (0.144 nm), then excellent agreement between the tight-binding model (see insert in Figure 5b) and DFT (main part of Figure 5b) is obtained. This demonstrates that longer S-C and shorter O-C bond lengths compared with the C-C bond and the associated changes in their resonance integrals leads to the lower conductance of III (SO) compared with I (SS) and II (OO).

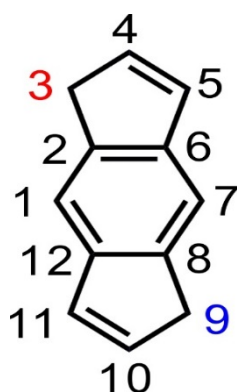


Figure 6. A tight binding representation of the isolated core of the benzodichalcogenophene molecule, with nearest neighbour coupling elements and on-site energies adjusted to account for the presence of heteroatoms on sites 3 and 9. In the tight-binding model, the hopping integrals of bonds 4-3, 2-3, 10-9 and 8-9 are adjusted to account for their altered bonds lengths.

Conclusions

In conclusion, we have carried out a combined experimental and theoretical study of the role of heteroatoms on electron transport through asymmetric and symmetric alkyne-terminated benzodichalcogenophene compounds. Excellent agreement between experiments, DFT-based theory and a minimal tight binding model is obtained. The tight-binding modelling of heteroatom substitution in these non-bipartite cores demonstrates that the lower conductance of the asymmetric molecule arises from the asymmetry induced by different bond lengths in the two 5-membered rings of the molecule. Furthermore, in the tight binding model, we find that it is necessary to account for the different overlap integrals of the C-O and C-S bonds, otherwise transport in the middle of the HOMO-LUMO gap would be the same for all molecules (compare figure S3 where overlap integrals are the same, with figure S4 where they are different). In essence, the atomic orbital energies of the heteroatoms and their bond strengths to neighbouring carbons both contribute to the tuning of QI in these molecules and both are needed to obtain agreement with experiment. As shown in Figure 4, the HOMO and LUMO orbital products of all molecules are of opposite sign and therefore, as confirmed by the absence of a destructive interference dip in their DFT transmission functions (Figure 5), their inter-orbital quantum interference is constructive^[35] and is resilient to heteroatom substitution.

Experimental Section

A Molecular Imaging PicoSPM was used to carry out the STM-BJ measurements under an argon atmosphere. Currents between 1 pA and 150 μ A were measured using a dual preamplifier and current-distance measurements were performed as described in^[46,47]. The electrode Au (polycrystalline) facet was subjected to electrochemical polishing before each measurement, annealed in a H₂ flame and then cooled under Ar. A freshly prepared 0.1 mM solution of the molecule was added to a Kel-F flow-through liquid cell mounted on top of the sample, and then tetrabutylammonium fluoride (TBAF) was added for cleavage of triisopropylsilyl groups.

FULL PAPER

WILEY-VCH

After moving the tip to a preset tunneling current of typically $iT = 50$ to 100 pA at $V_{bias} = 0.10$ V, the substrate was imaged. After fixing the lateral position of the tip and switching off the STM feedback, current-distance measurements were carried out by moving the tip towards the adsorbate-modified surface. The approach was stopped when the current reached typically 10 μ A. After a ~ 100 ms delay to allow tip relaxation and stable contact formation, the tip was retracted by 2 to 5 nm until the current reached a ~ 10 pA. These approaching and withdrawing actions were carried out at rates in the range 56 to 145 nm/s. To obtain meaningful statistics, up to 4000 traces were recorded for each set of experimental conditions.

Theoretical Section

Initially, the electronic structures of all molecules were computed at B3LYP level of theory with a 6-31G⁺⁺ basis set. Plots of the highest occupied and lowest unoccupied molecular orbitals (HOMO and LUMO, respectively) are shown in Figure 4.

To elucidate the experimentally observed trends, and to better evaluate the transport properties of these molecular junctions, calculations using a combination of DFT (the SIESTA code)^[48] and a non-equilibrium Green's function formalism were also carried out. This DFT-Landauer approach used in the modeling assumes that on the time scale taken by an electron to traverse the molecule, inelastic scattering is negligible. This is known to be an accurate assumption for molecules up to several nanometers in length.

For the transport calculations, each molecule was attached to opposing 35-atom (111) directed pyramidal gold electrodes, then geometrically optimization was carried out using the DFT code SIESTA, with a generalized gradient approximation^[48,49] (PBE functional), double ζ polarized basis set, 0.01 eV/Å force tolerance, a real-space grid with a plane wave cut-off energy of 250 Ry, zero bias voltage and 1 k points. When computing the optimal junction geometries, the molecules and first layers of gold atoms within each electrode were then allowed to relax. Then, eight layers of (111)-oriented bulk gold with each layer consisting of 6×6 atoms and a layer spacing of 0.235 nm were used to create the molecular junctions as shown in Figure 5(a). These layers were then further repeated to yield infinitely-long current-carrying gold electrodes. From these model junctions the transmission coefficient, $T(E)$, was calculated using the Gollum code.^[33] To determine E_F , the predicted conductance values of all molecules were compared with the experimental values and a single common value of E_F was chosen, which

gave the closest overall agreement. This yielded a value of $E_F - E_F^{DFT} = 1.0$ eV, which is close to the middle of the HOMO-LUMO gap and has been used in all of the theoretical results described previously. The use of DFT to compute the ground state energy of various molecular junctions, allows binding energies and optimal geometries to be computed. However, these calculations are subject to errors, due to the employing of localized basis sets, which are concentrated on the nuclei. At the point when atoms are sufficiently close to each other so that their basis functions overlap, can cause an artificial strengthening of the atomic interaction and an artificial shortening of the atomic distances. To avoid this kind of error the basis set superposition error correction (BSSE)^[50] or the counterpoise correction^[51] were used. Assuming two molecular systems, denoted a and b , the energy of the interaction may be expressed as:

$$\Delta E(ab) = E_{ab} - (E_a^{ab} + E_b^{ab})$$

The total energy of the combined a and b system is E_{ab} , while the total energies of isolated systems a and b are E_a and E_b respectively with keeping identical basis sets for the three energies. ΔE_{ab} is the binding energy between anchor groups and gold electrode.

Acknowledgements

We thank the National Natural Science Foundation of China (21503179, 21673195, 21722305, 21703188), the National Key R&D Program of China (2017YFA0204902), the Fundamental Research Funds for the Central Universities (Xiamen University: 20720170035) for funding work in Xiamen. Support from the UK EPSRC is acknowledged, through grant nos. EP/N017188/1, EP/P027156/1 and EP/N03337X/1. Support from the European Commission is provided by the H2020 project Bac-To-Fuel. Support from the Iraqi Ministry of Higher Education and Scientific Research is acknowledged.

Keywords: quantum interference • single-molecule conductors • density functional theory • scanning tunnelling microscopy • perturbation theory.

- [8] van der Molen, S. J.; Liao, J.; Kudernac, T.; Agutsson, J. S.; Bernard, L.; Calame, M.; van Wees, B. J.; Feringa, B. L.; Schönenberger, C. S. *Nano Lett.* 2009, 9, 76-80.
- [9] Jia, C. C.; Migliore, A.; Xin, N.; Huang, S. Y.; Wang, J. Y.; Yang, Q.; Wang, S. P.; Chen, H. L.; Wang, D. M.; Feng, B. Y.; Liu, Z. R.; Zhang, G. Y.; Qu, D. H.; Tian, H.; Ratner, M. A.; Xu, H. Q.; Nitzan, A.; Guo, X. F. *Science* 2016, 352, 1443-1445.
- [10] Frisenda, R.; Harzmann, G. D.; Celis Gil, J. A.; Thijssen, J. M.; Mayor, M.; van der Zant, H. S. J. *Nano Lett.* 2016, 16, 4733-4737.
- [11] Rincon-Garcia, L.; Ismael, A. K.; Evangelini, C.; Grace, I.; Rubio-Bollinger, G.; Porfyrakis, K.; Agrait, N.; Lambert, C. J. *Nat. Mater.* 2016, 15, 289-293.
- [12] Sadeghi, H.; Sangtarash, S.; Lambert, C. J. *Nano Lett.* 2015, 15, 7467-7472.
- [13] Kim, Y.; Jeong, W.; Kim, K.; Lee, W.; Reddy, P. *Nat. Nanotechnol.* 2014, 9, 881-885.
- [14] Baghernejad, M.; Zhao, X.; Baruel Orso, K.; Fuego, M.; Moreno-Garcia, P.; Rudnev, A. V.; Kaliginedi, V.; Veszteg, S.; Huang, C.; Hong, W.; Broekmann, P.; Wandlowski, T.; Thygesen, K. S.; Bryce, M. R. J. *Am. Chem. Soc.* 2014, 136, 17922-17925.
- [15] Geng, Y.; Sangtarash, S.; Huang, C.; Sadeghi, H.; Fu, Y.; Hong, W.; Wandlowski, T.; Decurtins, S.; Lambert, C. J.; Liu, S. X. *J. Am. Chem. Soc.* 2015, 137, 4469-4476; Sangtarash, S.; Huang, C.; Sadeghi, H.; Soroosh, G.; Hauser, J.; Wandlowski, T.; Hong, W.; Decurtins, S.; Liu, S.-X.; Lambert, C. J.; *J. Am. Chem. Soc.* 2015, 137 (35), 11425-11431.
- [16] Yang, G.; Wu, H.; Wei, J.; Zheng, J.; Chen, Z.; Liu, J.; Shi, J.; Yang, Y.; Hong, W. *Chin. Chem. Lett.* 2018, 29, 147-150.
- [17] Liu, X.; Sangtarash, S.; Reber, D.; Zhang, D.; Sadeghi, H.; Shi, J.; Xiao, Z.-Y.; Hong, W.; Lambert, C. J.; Liu, S.-X. *Angew. Chem. Int. Ed.* 2017, 56, 173-176.

References

- [1] Lambert, C. J. *Chem. Soc. Rev.* 2015, 44, 875-888.
- [2] Díez-Pérez, I.; Hihath, J.; Lee, Y.; Yu, L.; Adamska, L.; Kozhushner, M. A.; Oleynik, I. I.; Tao, N. *Nat Chem* 2009, 1, 635-641.
- [3] Yuan, L.; Breuer, R.; Jiang, L.; Schmittl, M.; Nijhuis, C. A. *Nano Lett.* 2015, 15, 5506-5512.
- [4] Batra, A.; Darancet, P.; Chen, Q. S.; Meisner, J. S.; Widawsky, J. R.; Neaton, J. B.; Nuckolls, C.; Venkataraman, L. *Nano Lett.* 2013, 13, 6233-6237.
- [5] Xu, B.; Xiao, X.; Yang, X.; Zang, L.; Tao, N. *J. Am. Chem. Soc.* 2005, 127, 2386-2387.
- [6] Song, H.; Kim, Y.; Jang, Y. H.; Jeong, H.; Reed, M. A.; Lee, T. *Nature* 2009, 462, 1039-1043.
- [7] Blum, A. S.; Kushmerick, J. G.; Long, D. P.; Patterson, C. H.; Yang, J. C.; Henderson, J. C.; Yao, Y.; Tour, J. M.; Shashidhar, R.; Ratna, B. R. *Nat. Mater.* 2005, 4, 167-172.

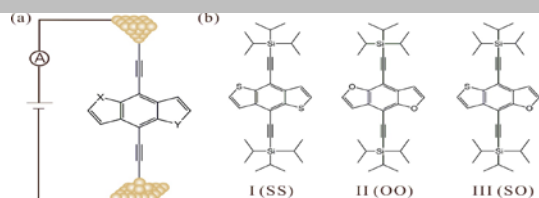
- [18] Feng Jiang, Douglas I. Trupp, Norah Algethami, Haining Zheng, Wenxiang He, Afaf Alqorashi, Chenxu Zhu, Chun Tang, Ruihao Li, Junyang Liu, Hatef Sadeghi, Jia Shi, Ross Davidson, Marcus Korb, Alexandre N. Sobolev, Masnun Naher, Sara Sangtarash, Paul J. Low, Wenjing Hong, Colin J. Lambert, *Angewandte Chemie* 2019, 131, 19163-19169.
- [19] Sören Bock, Oday Al-Owaedi, Samantha Eaves, David Milan, Mario Lemmer, Brian Skelton, Henry Osorio, Richard Nichols, Simon Higgins, Pilar Cea, Nicholas Long, Tim Albrecht, Santiago Martín, Colin Lambert, Paul J Low, *Chemistry-A European Journal* 2017, 23 (9), 2133-2143
- [20] Sangtarash, S.; Sadeghi, H.; Lambert, C. J. *Nanoscale* 2016, 8, 13199-13205.
- [21] Aeschi, Y.; Li, H.; Cao, Z.; Chen, S.; Amacher, A.; Bieri, N.; Oezen, B.; Hauser, J.; Decurtins, S.; Tan, S.; Liu, S.-X. *Org. Lett.* 2013, 15, 5586-5589.
- [22] Yi, C. Y.; Blum, C.; Lehmann, M.; Keller, S.; Liu, S. X.; Frei, G.; Neels, A.; Hauser, J.; Schürch, S.; Decurtins, S. *J. Org. Chem.* 2010, 75, 3350-3357.
- [23] Didane, Y.; Mehl, G. H.; Kumagai, A.; Yoshimoto, N.; Vidélot-Ackermann, C.; Brisset, H. J. *Am. Chem. Soc.* 2008, 130, 17681-17683.
- [24] Chen, H.-Y.; Hou, J.; Zhang, S.; Liang, Y.; Yang, G.; Yang, Y.; Yu, L.; Wu, Y.; Li, G. *Nat. Photonics* 2009, 3, 649-653.
- [25] Li, H.; Jiang, P.; Yi, C.; Li, C.; Liu, S.-X.; Tan, S.; Zhao, B.; Braun, J.; Meier, W.; Wandlowski, T.; Decurtins, S. *Macromolecules* 2010, 43, 8058-8062.
- [26] Zhou, J.; Wan, X.; Liu, Y.; Zuo, Y.; Li, Z.; He, G.; Long, G.; Ni, W.; Li, C.; Su, X.; Chen, Y. *J. Am. Chem. Soc.* 2012, 134, 16345-16351.
- [27] Li, Z.; Li, H.; Chen, S.; Froehlich, T.; Yi, C.; Schonenberger, C.; Calame, M.; Decurtins, S.; Liu, S.-X.; Borguet, E. *J. Am. Chem. Soc.* 2014, 136, 8867-8870.
- [28] Li, H.; Yi, C.; Moussi, S.; Liu, S.-X.; Daul, C.; Graetzel, M.; Decurtins, S. *RSC Adv.* 2013, 3, 19798-19801
- [29] Li, H.; Tang, P.; Zhao, Y.; Liu, S.-X.; Aeschi, Y.; Deng, L.; Braun, J.; Zhao, B.; Liu, Y.; Tan, S.; Meier, W.; Decurtins, S. *J. Polym. Sci. Part A: Polym Chem.* 2012, 50, 2935-2943.
- [30] Cheng, Z. L.; Skouta, R.; Vazquez, H.; Widawsky, J. R.; Schneebeli, S.; Chen, W.; Hybertsen, M. S.; Breslow, R.; Venkataraman, L. *Nat. Nanotechnol.* 2011, 6, 353-357.
- [31] Hong, W.; Li, H.; Liu, S.-X.; Fu, Y.; Li, J.; Kaliginedi, V.; Decurtins, S.; Wandlowski, T. *J. Am. Chem. Soc.* 2012, 134, 19425-19431; C. Huang et al., *Angew. Chem. Int. Ed.* 2015, 54, 14304-14307
- [32] Xu, B.; Tao, N. *J. Science* 2003, 301, 1221-1223.
- [33] Ferrer, J.; Lambert, C. J.; García-Suárez, V. M.; Manrique, D. Z.; Visontai, D.; Oroszlany, L.; Rodríguez-Ferradas, R.; Grace, I.; Bailey, S. W. D.; Gillemot, K.; Sadeghi, H.; Algharagholy, L. A. *New J. Phys.* 2014, 16, 093029.
- [34] Becke, A. D. *J. Chem. Phys.* 1993, 98, 5648-5652.
- [35] Lambert, C. J.; Liu, S.-X. *Chem. Eur. J.* 2018, 24, 4193-4201; K. Yoshizawa, T. Tada, and A. Staykov, *J. Am. Chem. Soc.* 130, 9406 (2008); X. Li, A. Staykov, and K. Yoshizawa, *J. Phys. Chem. C* 114, 9997 (2010); Y. Tsuji, A. Staykov, and K. Yoshizawa, *J. Am. Chem. Soc.* 133, 5955 (2011)
- [36] Stadler, R.; Jacobsen, K. W. *Phys. Rev. B* 2006, 74, 161405.
- [37] Al-Owaedi, O. A.; Milan, D. C.; Oerthel, M.-C.; Bock, S.; Yufit, D. S.; Howard, J. A. K.; Higgins, S. J.; Nichols, R. J.; Lambert, C. J.; Bryce, M. R.; Low, P. J. *Organometallics* 2016, 35, 2944-2954.
- [38] Yang, Y.; Liu, J.; Feng, S.; Wen, H.; Tian, J.; Zheng, J.; Schöllhorn, B.; Amatore, C.; Chen, Z.; Tian, Z. *Nano Res.* 2016, 9, 560-570.
- [39] Markussen, T.; Settnes, M.; Thygesen, K. S. *J. Chem. Phys.* 2011, 135, 144104
- [40] Milan, D. C.; Al-Owaedi, O. A.; Oerthel, M.-C.; Marqués-González, S.; Brooke, R. J.; Bryce, M. R.; Cea, P.; Ferrer, J.; Higgins, S. J.; Lambert, C. J.; Low, P. J.; Manrique, D. Z.; Martin, S.; Nichols, R. J.; Schwarzacher, W.; García-Suárez, V. M. *J. Phys. Chem. C* 2015, 120, 15666-15674.
- [41] Schwarz, F.; Kastlunger, G.; Lissel, F.; Riel, H.; Venkatesan, K.; Berke, H.; Stadler, R.; Lortscher, E. *Nano Lett.* 2014, 14, 5932-5940.
- [42] Sugimoto, K.; Tanaka, Y.; Fujii, S.; Tada, T.; Kiguchi, M.; Akita, M. *Chem Commun (Camb)* 2016, 52, 5796-5799.
- [43] Adak, O., et al., *Nano Letters*, 2015, 15(6): p. 3716-3722.
- [44] Sugimoto, K.; Tanaka, Y.; Fujii, S.; Tada, T.; Kiguchi, M.; Akita, M. *Chem Commun (Camb)* 2016, 52, 5796-5799.
- [45] Wen, H.-M.; Yang, Y.; Zhou, X.-S.; Liu, J.-Y.; Zhang, D.-B.; Chen, Z.-B.; Wang, J.-Y.; Chen, Z.-N.; Tian, Z.-Q. *Chem. Sci.* 2013, 4, 2471-2477.
- [46] Hong, W.; Valkenier, H.; Meszaros, G.; Manrique, D. Z.; Mishchenko, A.; Putz, A.; Garcia, P. M.; Lambert, C. J.; Hummelen, J. C.; Wandlowski, T. *Beilstein J. Nanotechnol.* 2011, 2, 699-713.
- [47] Yang, Y.; Gantenbein, M.; Alqorashi, A.; Wei, J.; Sangtarash, S.; Hu, D.; Sadeghi, H.; Zhang, R.; Pi, J.; Chen, L.; Huang, X.; Li, R.; Liu, J.; Shi, J.; Hong, W.; Lambert, C. J.; Bryce, M. R. *J. Phys. Chem. C* 2018, 122, 14965-14970.
- [48] Soler, J. e. M.; Artacho, E.; Gale, J. D.; García, A.; Junquera, J.; Ordejón, P.; Sánchez-Portal, D. *J. Phys-Condens. Mat.* 2002, 14, 2745-2779.
- [49] Artacho, E.; Anglada, E.; Dieguez, O.; Gale, J. D.; Garcia, A.; Junquera, J.; Martin, R. M.; Ordejon, P.; Pruneda, J. M.; Sanchez-Portal, D.; Soler, J. M. *J. Phys-Condens. Mat.* 2008, 20, 064208.
- [50] Jansen, H. B.; Ros, P. *Chem. Phys. Lett.* 1969, 3, 140-143.
- [51] Boys, S. F.; Bernardi, F. *Mol. Phys.* 1970, 19, 553-566.

Entry for the Table of Contents (Please choose one layout)

Layout 1:

FULL PAPER

Text for Table of Contents



Masoud Baghernejad^[a, c], Yang Yang^{#[a]}, Oday A. Al-Owaedi^{#[b]}, Yves Aeschi^[c], Biao-Feng Zeng^[a], Zahra Murtada Abd Dawood^[b], Xiaohui Li^[a], Junyang Liu^[a], Jia Shi^[a], Silvio Decurtins^[c], Shi-Xia Liu^[c], Wenjing Hong^[a, c] and Colin J. Lambert^{*[d]}

Page No. 1– Page No.6

Constructive Quantum
Interference in Single-Molecule
Benzodichalcogenophene